Video Article

Sub-acute Cerebral Microhemorrhages Induced by Lipopolysaccharide Injection in Rats

Dandan Li*[1,2], Hóngyi Zhào*[2,3], Wei Wei[2], Nan Liu[2], Yonghua Dr. Huang[2]

[1]Department of Neurology, Second Hospital of Shanxi Medical University

[2]Department of Neurology, PLA Army General Hospital

[3]Department of Neurology, NO 261 Hospital of PLA

*These authors contributed equally

Correspondence to: Yonghua Dr. Huang at huangyonghua2017@126.com

URL: https://www.jove.com/video/58423
DOI: doi:10.3791/58423

Keywords: Neuroscience, Issue 140, Blood-brain barrier, cerebral microhemorrhages, lipopolysaccharide, neuroinflammation, rats, protocol

Date Published: 10/17/2018

Citation: Li, D., Zhào, H., Wei, W., Liu, N., Dr. Huang, Y. Sub-acute Cerebral Microhemorrhages Induced by Lipopolysaccharide Injection in Rats. *J. Vis. Exp.* (140), e58423, doi:10.3791/58423 (2018).

Abstract

Cerebral microhemorrhages (CMHs) are common in aged patients and are correlated to various neuropsychiatric disorders. The etiology of CMHs is complex, and neuroinflammation is often observed as a co-occurrence. Here, we describe a sub-acute CMHs rat model induced by lipopolysaccharide (LPS) injection, as well as a method for detecting CMHs. Systemic LPS injection is relatively simple, economical, and cost-effective. One major advantage of LPS injection is its stability to induce inflammation. CMHs caused by LPS injection could be detected by gross observation, hematoxylin and eosin (HE) staining, Perl's Prussian staining, Evans blue (EB) double-labeling, and magnetic resonance imaging-susceptibility weighted imaging (MRI-SWI) technology. Finally, other methods of developing CMHs animal models, including their advantages and/or disadvantages, are also discussed in this report.

Video Link

The video component of this article can be found at https://www.jove.com/video/58423/

Introduction

Classical cerebral microhemorrhages (CMHs) refer to tiny perivascular deposits of blood degradation products such as hemosiderin from red blood cells in the brain[1]. According to the Rotterdam Scan Study, CMHs could be found in nearly 17.8% of persons aged 60–69 years and 38.3% in those over 80 years[2]. The prevalence of CMHs in the elderly is relatively high, and a correlation between the accumulation of CMHs and cognitive and neuropsychiatric dysfunction has been established[3,4]. Several animal models of CMHs have recently been reported, including rodent models induced by type IV collagenase stereotaxic injection[5], APP transgenic[6], β-N-methylamino-L-alanine exposure[7], and hypertension[8], with CMHs induced by systemic inflammation as one of the most well-accepted choices. Fisher *et al.*[9] first used LPS derived from *Salmonella typhimurium* to develop an acute CMHs mouse model. Subsequently, the same group reported the development of a sub-acute CMHs mouse model using the same approach[2].

LPS is considered as a standardized inflammatory stimulus *via* intraperitoneal injection. Previous studies have confirmed that LPS injection could cause neuroinflammation as reflected by large amounts of microglia and astrocyte activation in animal models[2,10]. Furthermore, a positive correlation between activation of neuroinflammation activation and the number of CMHs has been established[2,10]. Based on these previous studies, we were prompted to develop a CMHs rat model by intraperitoneal injection of LPS.

Advances in detection technologies have resulted in an increase in the number of research investigations on CMHs. The most widely acknowledged methods of detecting CMHs include the detection of red blood cells by hematoxylin and eosin (HE) staining, ferric iron detection by Prussian Blue staining[9], detection of Evans blue (EB) deposition by immunofluorescence imaging, and 7.0 Tesla magnetic resonance imaging-susceptibility weighted imaging (MRI-SWI)[10]. The present study aims to develop a method of screening for CMHs.

Protocol

All methods described here have been approved by the Animal Care and Use Committee (ACUC) of the PLA Army General Hospital.

1. Materials

1. Preparation of LPS injection

1. Add 25 mL of distilled water to 25 mg of LPS powder derived from *S. typhimurium* to a final concentration of 1 mg/mL. Store the injection in a sterile tube at 4 °C.
   CAUTION: LPS is toxic.
2. Prepare a 2% EB solution in normal 0.9% saline solution to keep EB injection at working concentration.

2. Animals

1. Administer LPS to male Sprague-Dawley (SD) rats, aged 10 weeks (average weight: 280 ± 20 g) by intraperitoneal injection.
   CAUTION: If rats are purchased from another organization, then the adaptive phase should not be less than 7 days.

3. LPS Injections

1. Inject LPS intraperitoneally into each rat at a dose of 1 mg/kg, and return the rats to their home cage.
   NOTE: Anesthesia is not necessary.
2. Six hours later, inject the same dose of LPS injection into the rats.
3. Sixteen hours later inject the same dose of LPS into the rats.
   CAUTION: Injecting SD rats with LPS at a dose of 1 mg/kg may result in a 5% mortality rate. The mortality rate could further increase in younger or older rats or pregnant female rats.
4. Return the rats to their cages after LPS injection and provide *ad libitum* access to food and drink.
   NOTE: Rats will exhibit a distinct systemic inflammatory response, and thus it is essential that the cages remain clean throughout the experiment. Rats should be frequently (2x day) monitoring for weight, general appearance and attitude after the first LPS injection. If the rats start to exhibit a hunched posture, unwillingness to move, significant weight loss (>20%), porphyrin staining that they be humanely euthanized prior to the 7 day EB study end point.

4. Sample Collection

1. EB injection
   1. Seven days after the first injection, anesthetize the rat by intraperitoneally according to your approved IACUC protocol.
   2. Wait 1–2 min until the rats do not show corneal reflex responses. Perform a 5–8 mm-deep cardiac puncture on each rat; the puncturing point should be 5 mm to the left margin of sternum at the 3rd and 4th intercostals space.
   3. Wait until blood recovery is observed, and then inject EB at a dose of 0.2 mL/100 g body weight into the left heart ventricle.
      CAUTION: Cardiac puncture and EB injection should be carefully performed. EB might be injected into thoracic cavity or pericardium instead of the left heart ventricle.
      1. Suck back with an empty tube and replace this volume with an EB tube before injection to help reduce the failure rate (*e.g.*, injection to rib cage by error).
   4. Keep the rat in a supine position for 10 min.
      NOTE: If sample is not used to detect EB leakage in immunofluorescence imaging, then this step may be omitted.
2. Gross observation
   1. Perform cardiac perfusions using ice-cold 1 M phosphate buffer saline (PBS) to clear the cerebral vasculature and brains.
      1. Using a scalpel, make an abdominal incision across the entire length of the diaphragm.
      2. Cut through ribs just left of the rib cage midline.
      3. Open up the thoracic cavity. Use clamps to expose the heart and to facilitate drainage of blood and other fluids.
      4. While steadily holding the heart with forceps (the heart should still be beating), directly insert a needle into the protrusion of the left ventricle to extend this to about 5 mm. Secure the needle at that position by clamping near the point of entry.
         CAUTION: Do not excessively extend the needle, as it can pierce the interior wall and compromise the circulation of solutions.
      5. Release the valve to allow the flow ice-cold PBS solution (200–300 mL) at a slow and steady rate at around 20 mL/min using a perfusion pump. If the animals require fixation instead of gross observation, then use the same dose of ice-cold 0.9% saline solution.
      6. Using sharp scissors, make an incision in the atrium, ensuring that the solution continuously flows. If the fluid does not flow freely or is coming from the animal's nostrils or mouth, reposition the needle.
   2. Screen for CMHs by gross observation.
      NOTE: If the sample is not used in calculating the number of CMHs by gross observation, then this step may be omitted.
3. Fixation
   1. Perform cardiac perfusions using ice-cold 0.9% saline solution (200–300 mL) to clear the cerebral vasculature and brains.
   2. Perform cardiac perfusions using ice-cold 4% paraformaldehyde for fixation.
   3. Decapitate the rat, isolate the brain, and immerse the brain in 20% sucrose solution for at least 6 h.
   4. Change the solution into 30% sucrose and fix for another 6 h.
4. Prepare 10 mm-thick brain tissues sections using a cryostat.

5. HE Staining

NOTE: This procedure is performed using a HE Staining Kit.

1. Wash the slides in distilled water.
2. Stain in hematoxylin solution for 8 min. Wash in running tap water for 5 min.
3. Differentiate in 1% acid alcohol for 30 s. Wash in running tap water for 1 min.
4. Stain in 0.2% ammonia water (Bluing) or saturated lithium carbonate solution for 30 s to 1 min. Wash in running tap water for 5 min.
5. Rinse in 95% alcohol (10 dips).
6. Counterstain with eosin solution for 30 s to 1 min.
7. Dehydrate through 95% alcohol, two changes of absolute alcohol, for 5 min each.
8. Clear in xylene for 30 s.
9. Mount using Liu's method[9].
10. Analyze using a brightfield fluorescence microscope.
    NOTE: Red blood cells released from blood vessels, which are the components of CMHs, appear in red-orange under HE staining.

6. Perl Prussian Blue Staining

NOTE: This procedure is performed using a Perls Staining Kit.

1. Wash slides with distilled water.
2. Stain in reaction solution with equal parts mixture of ferrocyanide and hydrochloric acid for 10 min.
3. Dehydrate, clear, mount, and analyze the slides as described in steps 5.7–5.10.

7. EB double-staining

NOTE: This procedure follows step 4.1.3.

1. Wash slides with PBS three times for 5 min each.
2. Incubate slides with 4',6-diamidino-2-phenylindole (DAPI) solution for 15 min at room temperature.
3. Wash the slides with PBS solution three times for 5 min each, and mount slides with PBS-glycerol solution.
4. Analyze images on a fluorescence microscope. EB deposition is indicated by red fluorescence; nuclei are indicated by blue fluorescence.

8. MRI-SWI

1. Perform MRI on a 7-T magnet equipped with an actively shielded gradient system (16 cm inner diameter).
2. Seven days after treatment, anesthetize the rats by facemask inhalation of 1.5–2.0% isoflurane using an isoflurane anesthesia system.
3. Apply vet ointment onto the eyes of the rat to prevent dryness while under anesthesia.
4. Keep the rats in prone position and perform an MRI-SWI scan.
5. Obtain SWI weighted scans using a fast-spin echo sequence using the following parameters: echo time (TE) 8 ms, repetition time (TR) 40 ms, flip angle=12°, field of view (FOV) 35 mm × 35 mm, acquisition matrix 384 × 384, to acquire 1 mm-thick slices.
6. Identify CMHs in MRI-SWI according to Greenberg *et al.*[11], which included the following criteria: (1) a diameter of ≤10 mm, and (2) circular, isolated, and low-signal intensity spots.
7. At the end of the experiment, euthanize the rats using the overdose carbon dioxide (at a flow of 6 L/min or 30% of the container volume) method.

Representative Results

CMHs can be detected using various approaches. The most well-accepted methods include the following: (1) gross observation and assessment of surface CMHs (shown in **Figure 1**, upper panel); (2) HE staining for the detection of red blood cells (shown in **Figure 2A**, upper panel) or Prussian staining detecting ferric iron derived from lysis of red blood cells (**Figure 2A**, lower panel); (3) EB doubled staining for the detection of EB deposition derived from BBB leakage (**Figure 3**, left panel); (4) MRI-SWI detection of CMHs hypointense signals (**Figure 4**, left panel).

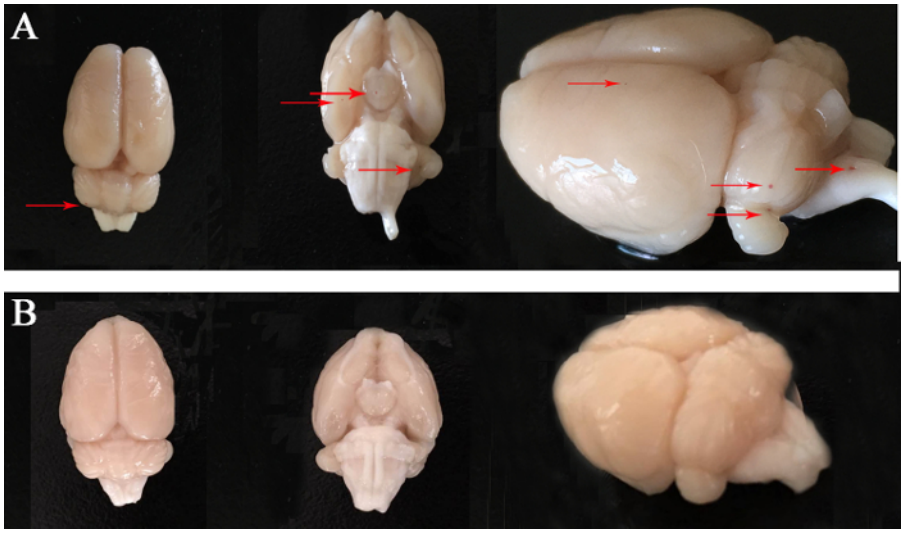

Figure 1: Gross observation of surface CMHs. Upper panel (**A**): Rat model; Lower panel (**B**): Control animal. Red arrows signify surface CMHs. Modified and reused with permission[10]. Please click here to view a larger version of this figure.

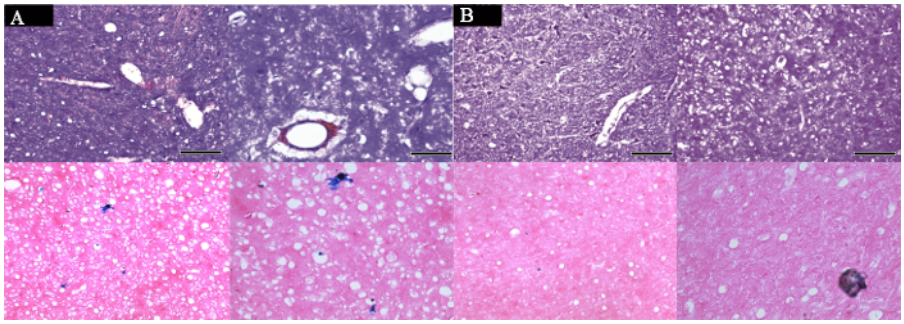

Figure 2: HE staining and Prussian staining images. (**A**) Reflected rat model. Red blood cells were found outside the capillaries in upper panel, and ferric iron points derived from lysis of red blood cells were detected in lower panel; (**B**) Reflected control animal. Neither red blood cells nor ferric iron points were found. Scale bars = 100 μm (left panel of A and B). Scale bars = 50 μm (right panel of A and B). Modified and reused with permission[10]. Please click here to view a larger version of this figure.

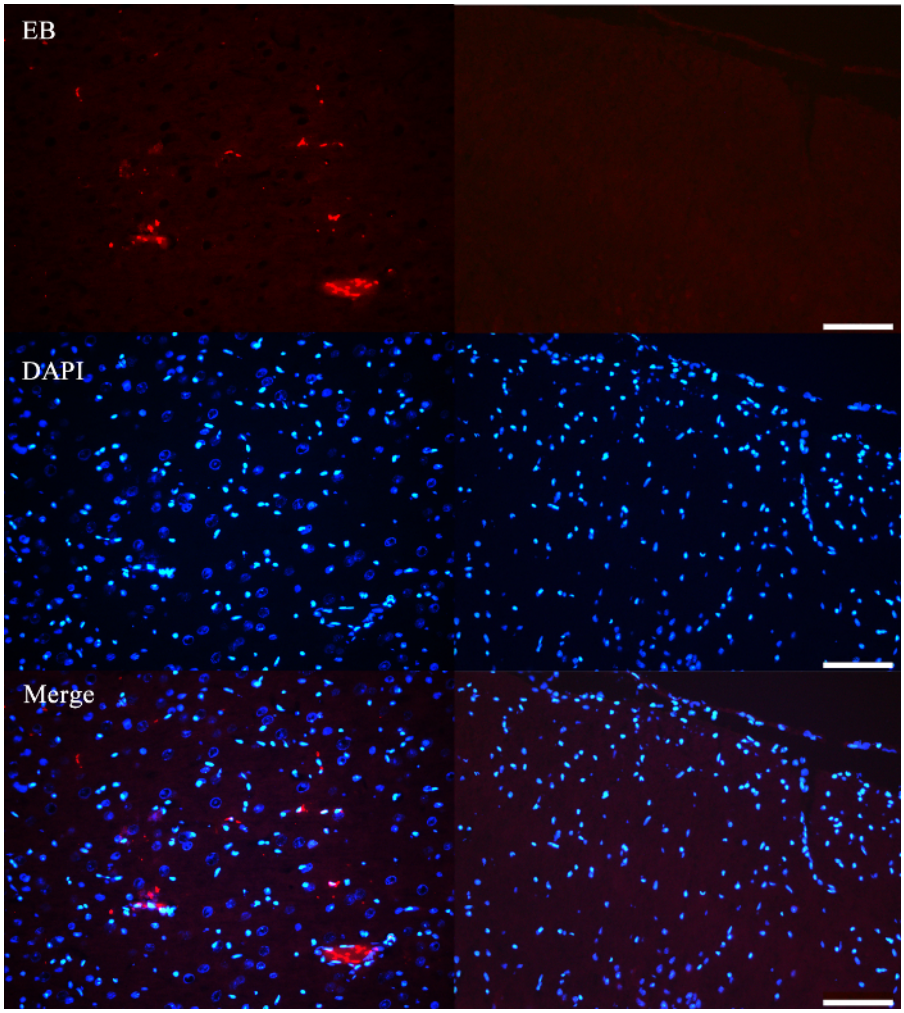

Figure 3. Double labeled EB deposition fluorescence imaging. Left panel: Rat model. Amount of EB molecules leaked from injured BBB were detected (in red); Right panel: Control animal. No EB molecules were detected. DAPI in blue was used as mount medium. Scale bars = 100 μm. Modified and reused with permission[10]. Please click here to view a larger version of this figure.

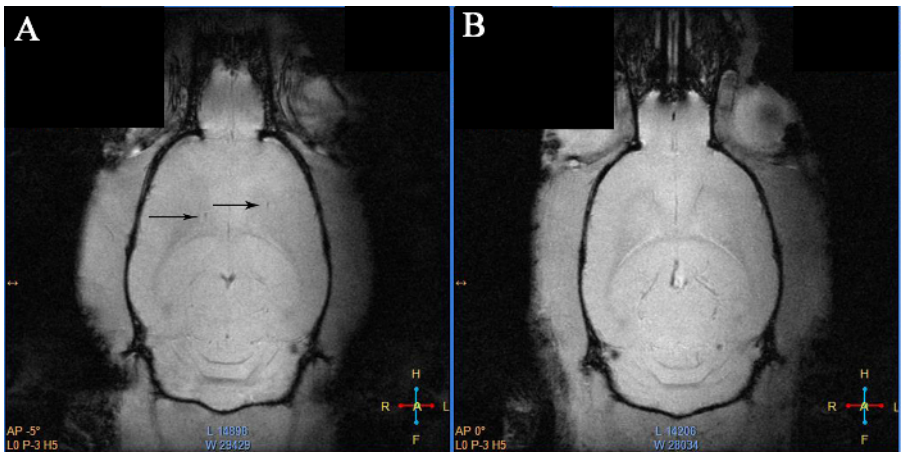

Figure 4. MRI-SWI images. Left panel (**A**): Rat model. Black arrows signify hypointense signals of CMHs; Right panel (**B**): Control animal. No hypointense signals were found. Modified and reused with permission[10]. Please click here to view a larger version of this figure.

Discussion

Research studies on CMHs have increased in the past few years. However, the mechanism of CMHs remains unclear, prompting scientists to establish animal models that simulate this particular condition. For example, Hoffmann *et al.* developed a hypoxia-induced CMHs mouse model that shows that CMHs are caused by hypoxia and disruption of cerebrovascular autoregulation[12]. Reuter *et al.*[5] established a CMHs model in

APP23-transgenic mice, which showed that cerebral amyloid angiopathy (CAA) plays a major role in the etiology of CMHs. Fisher *et al.* reported a CMHs mouse model that was induced by LPS injection[9], which revealed that CMHs are caused by inflammation[2,13,14]. Similarly, we have successfully developed a sub-acute CMHs model in SD rats using LPS injection and have found that nitric oxide synthase (NOS), especially neural NOS and endothelial NOS, are involved in the etiology of CMHs, which result in inflammation[10].

The critical step of our protocol is the LPS injection, which has been extensively used in developing murine models of neuropsychiatric disorders such as depression[15], schizophrenia[16], Parkinson's disease[17], Alzheimer's disease[18], and Prion disease[19]. To our knowledge, our use of a single dose (1 mg/kg) is much higher than that was applied in other studies[15,16,17,18,19]. This might be a plausible reason for the mortality in the current study. LPS dose modification for CMHs induction may be an interesting research topic, as different doses or injection schedule have been shown to influence the number, size, distribution, and progression of CMHs[2]. A previous study has shown that the administration of LPS to mice at a dose of 3 mg/kg induces acute CMHs[2].

Although the development of different animal models has facilitated research investigations on CMHs, we have to admit that those animal models do not simulate the process of clinical CMHs. For example, in our rat model, as well as Fisher's mice model, CMHs were observed in the cerebellum, although most were observed in lobar regions (mainly CAA-related) and deep- or infra-tentorial locations (mainly hypertension-related)[20,21]. We have no explanation for this discrepancy in distribution, although both Fisher and our team attribute this observation to the vulnerability of cerebellar blood vessels to inflammation.

In most clinical cases, CMHs result from more than one etiological factor, although inflammation plays an important role in its etiology. Studies focusing on multiple factors that induce CMHs, instead of pure inflammation-induced CMHs, can thus be more helpful in simulating this condition. The LPS injection model could be used with other underlying factors to investigate the mechanism of CMHs. For example, Fisher *et al.* have conducted a preliminary, yet interesting step with aging mice injected with LPS, and demonstrated that aging is a key factor that could make the brain more susceptible to inflammation-induced CMHs[14]. In our opinion, the significance of the present model is its compatibility with other factors in animal models for aging[14], trauma[22], as well as chronic diseases such as hypercholesterolemia[23], or transgenic models such as hypertension[24] because of the simplicity, time-effectiveness, and stability of this protocol.

Patients with CMHs show cognitive declines, neuropsychiatric manifestations, and vertigo, which are associated with the distribution of CMHs. One limitation of the present protocol is that after LPS injection, we could not rule out the effects of peripheral inflammation on the behavior of the rats, although a decrease in social behavior and burrowing (intrinsic natural activity of rodent reflecting the impairment of daily activities) were observed. Further studies on ways to improve our method of generating a CMHs animal model, *e.g.,* method of injecting LPS or schedule of observation, are warranted.

Nevertheless, this simple, cost-effective, and stable CMHs murine model induced by LPS injection may be utilized by researchers in elucidating the etiology of CMHs.

Disclosures

The authors have nothing to disclose.

Acknowledgements

We thank Teacher Jian Feng Lei and colleagues from Capital Medical University for guidance during MRI. We also thank Jing Zeng from the Department of Neurology, the Second People's Hospital of Yichang for providing technical support.

References

1. Sumbria, R.K., *et al.* A murine model of inflammation-induced cerebral microbleeds. *J Neuroinflammation.* **13** (1), 218 (2016).
2. Vernooij, M.W., *et al.* Prevalence and risk factors of cerebral microbleeds: the Rotterdam Scan Study. *Neurology.* **70** (14), 1208-1214 (2009).
3. Pettersen, J.A., *et al.* Microbleed topography, leukoaraiosis, and cognition in probable Alzheimer disease from the Sunnybrook dementia study. *Archives of Neurology.* **65** (6), 790-795 (2008).
4. Xu, X., *et al.* Cerebral microbleeds and neuropsychiatric symptoms in an elderly Asian cohort. *Journal of Neurology, Neurosurgery, and Psychiatry.* **88** (1), 7-11 (2017).
5. Mcauley, G., Schrag, M., Barnes, S., Obenaus, A., Dickson, A., Kirsch, W. In vivo iron quantification in collagenase-induced microbleeds in rat brain. *Magnetic Resonance in Medicine.* **67** (3), 711-717 (2012).
6. Reuter, B., *et al.* Development of cerebral microbleeds in the APP23-transgenic mouse model of cerebral amyloid angiopathy-a 9.4 tesla MRI study. *Frontiers in Aging Neuroscience.* **8** (8), 170 (2016).
7. Scott, L.L., Downing, T.G. A single neonatal exposure to BMAA in a rat model produces neuropathology consistent with neurodegenerative diseases. *Toxins.* **10** (1), E22 (2018).
8. Toth, P., *et al.* Aging exacerbates hypertension-induced cerebral microhemorrhages in mice: role of resveratrol treatment in vasoprotection. *Aging Cell.* **14** (3), 400-408 (2015).
9. Liu, S., *et al.* Comparative analysis of H&E and Prussian blue staining in a mouse model of cerebral microbleeds. *Journal of Histochemistry & Cytochemistry.* **62** (11), 767-773 (2014).
10. Zeng, J., Zhào, H., Liu, Z., Zhang, W., Huang, Y. Lipopolysaccharide induces subacute cerebral microhemorrhages with involvement of Nitric Oxide Synthase in rats. *Journal of Stroke and Cerebrovascular Diseases.* **27** (7), 1905-1913 (2018).
11. Greenberg, S.M., *et al.* Cerebral microbleeds: A guide to detection and interpretation. *Lancet Neurology.* **8** (2), 165-174 (2009).
12. Hoffmann, A., *et al.* High-Field MRI reveals a drastic increase of hypoxia-induced microhemorrhages upon tissue reoxygenation in the mouse brain with strong predominance in the olfactory bulb. *Plos One.* **11** (2), e0148441 (2016).

13. Sumbria, R.K., *et al.* Effects of phosphodiesterase 3A modulation on murine cerebral microhemorrhages. *Journal of Neuroinflammation.* **14** (1), 114 (2017).
14. Sumbria, R.K., *et al.* Aging exacerbates development of cerebral microbleeds in a mouse model. *Journal of Neuroinflammation.* **15** (1), 69 (2018).
15. Mello, B.S.F., *et al.* Sex influences in behavior and brain inflammatory and oxidative alterations in mice submitted to lipopolysaccharide-induced inflammatory model of depression. *Journal of Neuroimmunol.* **320**, 133-142 (2018).
16. Souza, D.F.D., *et al.* Changes in astroglial markers in a maternal immune activation model of schizophrenia in Wistar rats are dependent on sex. *Frontiers in Cellular Neuroscience.* **9** (489) (2015).
17. Dutta, G., Zhang, P., Liu, B. The Lipopolysaccharide Parkinson's disease animal model: mechanistic studies and drug discovery. *Fundamental & Clinical Pharmacology.* **22** (5), 453-464 (2008).
18. El-Sayed, N.S., Bayan, Y. Possible role of resveratrol targeting estradiol and neprilysin pathways in lipopolysaccharide model of Alzheimer disease. *Advances in Experimental Medicine and Biology.* **822** (822), 107-118 (2015).
19. Combrinck, M.I., Perry, V.H., Cunningham, C. Peripheral infection evokes exaggerated sickness behaviour in pre-clinical murine prion disease. *Neuroscience.* **112** (1), 7-11 (2002).
20. Pantoni, L., Cerebral small vessel disease: from pathogenesis and clinical characteristics to therapeutic challenges. *Lancet Neurology.* **9** (7), 689-701 (2010).
21. Rosand, J., *et al.* Spatial clustering of hemorrhages in probable cerebral amyloid angiopathy. *Annals of Neurology.* **58** (3), 459-462 (2005).
22. Robinson, S., *et al.* Microstructural and microglial changes after repetitive mild traumatic brain injury in mice. *Journal of Neuroscience Research.* **95** (4), 1025-1035 (2017).
23. Kraft, P., *et al.* Hypercholesterolemia induced cerebral small vessel disease. *Plos One.* **12** (8), e0182822 (2017).
24. Schreiber, S., Bueche, C.Z., Garz, C., Baun, H. Blood brain barrier breakdown as the starting point of cerebral small vessel disease? - New insights from a rat model. *Experimental & Translational Stroke Medicine.*, **5** (1), 4 (2013).

